

Studies of charmless B decays including CP violation effects

IRINA NASTEVA¹

*Centro Brasileiro de Pesquisas Físicas
Rio de Janeiro, Brazil*

The latest experimental results in charmless B decays are presented with a focus on CP violation measurements. These include the first observation of CP violation in B_s^0 decays, evidence for CP violation in charmless three-body B^\pm decays, branching fraction measurements of $B^\pm \rightarrow p\bar{p}K^\pm$ decays and the first observation of the decay $B_s^0 \rightarrow \phi\bar{K}^{*0}$ from LHCb, a comparison of $B^\pm \rightarrow K^+K^-K^\pm$ CP violation measurements between LHCb and BaBar, and the first evidence for the decay $B^0 \rightarrow K^+K^-\pi^0$ obtained by Belle.

PRESENTED AT

Flavor Physics and CP Violation 2013 (FPCP–2013)
Buzios, Rio de Janeiro, Brazil, May 19–24, 2013

¹On behalf of the LHCb collaboration.

1 Introduction

Charmless B decays occur through loop diagrams and are thus sensitive to possible new physics contributions in the loops. Two- and three-body charmless B decays proceed via CP -conserving penguin diagrams and CP -violating tree diagrams with $b \rightarrow u$ transitions, which give access to the γ CKM angle. The tree-penguin interference allows to look for direct CP violation in $B_{(s)}^0 \rightarrow hh'$ and $B^\pm \rightarrow hhh'$ decays, where h and h' stand for hadrons. The direct CP asymmetry of B decays to a final state f is defined as

$$A_{CP}(B \rightarrow f) = \frac{\Gamma(\overline{B} \rightarrow \overline{f}) - \Gamma(B \rightarrow f)}{\Gamma(\overline{B} \rightarrow \overline{f}) + \Gamma(B \rightarrow f)}. \quad (1)$$

With the LHCb experiment [1] currently running, and BaBar [2] and Belle [3] analysing their full datasets, we present several new and recent results of CP violation and branching fraction measurements of charmless B decays. The LHCb results are obtained from 1 fb^{-1} of data from pp collisions at a centre-of-mass energy of $\sqrt{s} = 7 \text{ TeV}$. Section 2 presents the LHCb measurements of CP violation in charmless two-body $B_{(s)}^0$ decays. Section 3 details the results of studies of charmless three-body decays, including CP violation measurements of $B^\pm \rightarrow K^\pm \pi^+ \pi^-$, $B^\pm \rightarrow K^\pm K^+ K^-$, $B^\pm \rightarrow K^+ K^- \pi^\pm$ and $B^\pm \rightarrow \pi^+ \pi^- \pi^\pm$ from LHCb, a comparison of the $B^\pm \rightarrow K^\pm K^+ K^-$ results with BaBar, evidence for a new decay channel $B^0 \rightarrow K^+ K^- \pi^0$ from Belle, and branching fraction measurements of $B^\pm \rightarrow p\bar{p}K^\pm$ decay components from LHCb. Finally, Section 4 describes the observation of the decay to two vector mesons $B_s^0 \rightarrow \phi \overline{K}^{*0}$ by LHCb.

2 Charmless two-body $B_{(s)}^0$ decays

The LHCb experiment has recently measured the direct CP -violating asymmetries of the decays $B^0 \rightarrow K^+ \pi^-$ and $B_s^0 \rightarrow K^- \pi^+$ with an unprecedented precision [4]. The data samples of two-body decays are selected using two different sets of criteria aimed at obtaining the best sensitivity to A_{CP} for B^0 and B_s^0 decays, respectively. The B_s^0 measurement requires a stronger rejection of combinatorial backgrounds, due to the lower probability for a b quark to form a B_s^0 meson. After the kinematic and trigger selections, the two data samples are subdivided into different final states, using particle identification (PID) information [5]. The PID selection criteria applied to B_s^0 candidates are tighter than those for the B^0 sample. In order to determine the background contributions with one or more misidentified final-state particles (cross-feed backgrounds), the PID efficiencies and misidentification rates are determined from large samples of calibration data, containing $D^{*+} \rightarrow D^0(K^- \pi^+) \pi^+$ and $\Lambda \rightarrow p \pi^-$ decays.

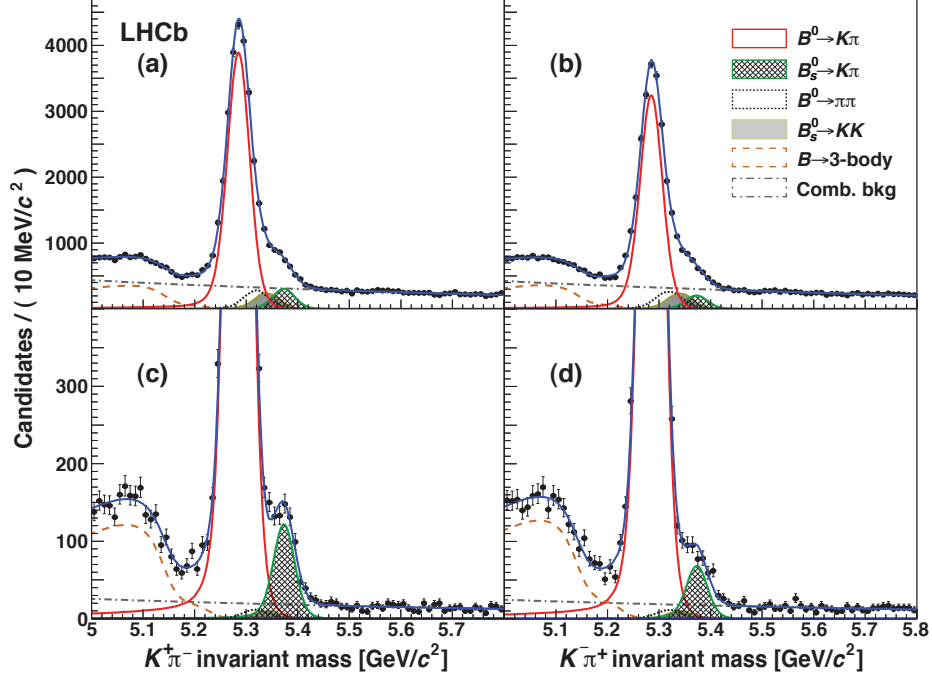


Figure 1: Invariant mass spectra using the event selection optimised for (a, b) $A_{CP}(B^0 \rightarrow K^+\pi^-)$ and (c, d) $A_{CP}(B_s^0 \rightarrow K^-\pi^+)$. Panels (a) and (c) show the $K^+\pi^-$ invariant mass and panels (b) and (d) show the $K^-\pi^+$ invariant mass. The results of the unbinned maximum likelihood fits are overlaid.

The signal yields and raw asymmetries are obtained from unbinned extended maximum likelihood fits to the invariant mass spectra of the selected candidates, shown in Fig. 1. The raw asymmetries are corrected for detection asymmetry effects due to detector reconstruction, acceptance and final-state particle interaction with matter, and for the $B_{(s)}^0 - \bar{B}_{(s)}^0$ production asymmetry. The CP asymmetry is calculated as

$$A_{CP} = A_{\text{raw}} - A_{\Delta}, \quad (2)$$

where the correction A_{Δ} is the sum of the detection asymmetry $A_D(K\pi)$ and the production asymmetry $A_P(B_{(s)}^0)$:

$$A_{\Delta} = \zeta_{d(s)} A_D(K\pi) + \kappa_{d(s)} A_P(B_{(s)}^0) \quad (3)$$

with $\zeta_d = 1$, $\zeta_s = -1$ and $\kappa_{d(s)}$ are dilution factors due to mixing.

The detection asymmetries are determined from data using $D^{*+} \rightarrow D^0(K^-\pi^+)\pi^+$ and $D^{*+} \rightarrow D^0(K^+K^-)\pi^+$ decays. From their time-integrated asymmetries the values $A_D(K\pi) = (-1.15 \pm 0.23)\%$ for $B^0 \rightarrow K^+\pi^-$ and $A_D(K\pi) = (-1.22 \pm 0.21)\%$ for $B_s^0 \rightarrow K^-\pi^+$ decays are measured. The production asymmetries are taken from a

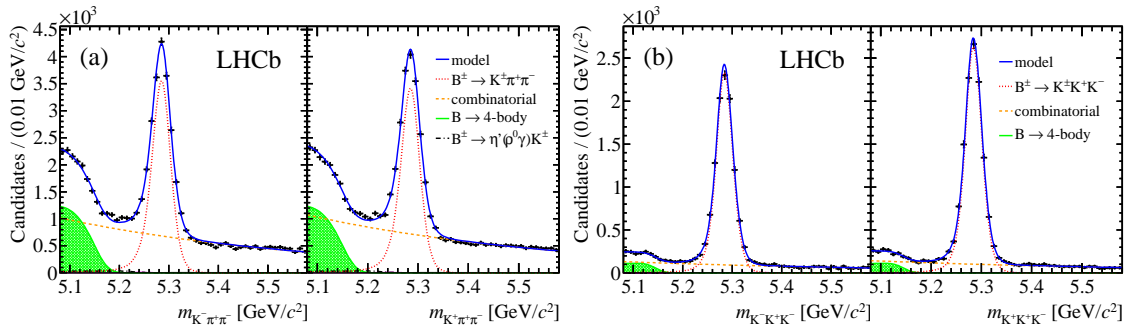


Figure 2: Invariant mass spectra of (a) $B^\pm \rightarrow K^\pm \pi^+ \pi^-$ and (b) $B^\pm \rightarrow K^\pm K^+ K^-$ decays. The left (right) panels show the B^- (B^+) modes. The results of the unbinned maximum likelihood fits are overlaid.

time-dependent fit to the decay rate and asymmetry of the B^0 and B_s^0 samples, obtaining $A_P(B^0) = (0.1 \pm 1.0)\%$ and $A_P(B_s^0) = (4 \pm 8)\%$. Finally, the CP asymmetries of $B_{(s)}^0 \rightarrow K\pi$ decays are measured to be

$$\begin{aligned} A_{CP}(B^0 \rightarrow K^+ \pi^-) &= -0.080 \pm 0.007 (\text{stat}) \pm 0.003 (\text{syst}), \\ A_{CP}(B_s^0 \rightarrow K^- \pi^+) &= 0.27 \pm 0.04 (\text{stat}) \pm 0.01 (\text{syst}). \end{aligned}$$

The systematic uncertainties account for the PID calibration, the signal and background fit models, and the detection charge asymmetries. The significances of the results, calculated by dividing the central values by the sum in quadrature of the statistical and systematic uncertainties, are 10.5σ and 6.5σ , respectively. The former is the most precise measurement of $A_{CP}(B^0 \rightarrow K^+ \pi^-)$, and the latter represents the first observation of direct CP violation in the B_s^0 system.

3 Charmless three-body B decays

3.1 CP violation in $B^\pm \rightarrow K^\pm \pi^+ \pi^-$ and $B^\pm \rightarrow K^\pm K^+ K^-$ decays

Decays of the type $B^\pm \rightarrow h^+ h^- h'^\pm$ ($h, h' = K, \pi$) offer the possibility to study CP violation patterns in the Dalitz plane in addition to the global asymmetries. CP violation can appear through the penguin-tree interference, through intermediate resonant states or through final-state hadron rescattering [6, 7, 8, 9] between two or more channels with the same flavour quantum numbers, such as $B^\pm \rightarrow K^\pm \pi^+ \pi^-$ and $B^\pm \rightarrow K^\pm K^+ K^-$. The latter effect, also called “compound CP violation” [10], is constrained by CPT invariance so that the sum of all partial decay widths of a particle, to channels with the same final-state quantum numbers, must match those of its antiparticle. The joint study of $B^\pm \rightarrow K^\pm \pi^+ \pi^-$ and $B^\pm \rightarrow K^\pm K^+ K^-$ decays was motivated by their CPT connection.

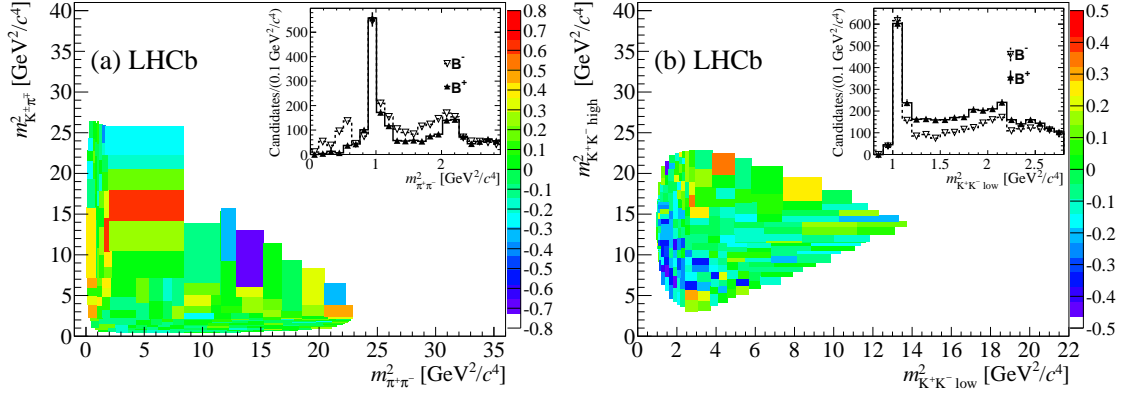


Figure 3: Raw asymmetries in bins of the Dalitz plot for (a) $B^\pm \rightarrow K^\pm \pi^+ \pi^-$ and (b) $B^\pm \rightarrow K^\pm K^+ K^-$. The inset plots show the projections of the number of background-subtracted events in bins of (a) the $m_{\pi^+ \pi^-}^2$ variable for $m_{K^\pm \pi^\mp}^2 < 15 \text{ GeV}^2/c^4$ and (b) the $m_{K^+ K^- \text{ low}}^2$ variable for $m_{K^+ K^- \text{ high}}^2 < 15 \text{ GeV}^2/c^4$.

The LHCb collaboration presented for the first time a measurement of the direct CP asymmetry in $B^\pm \rightarrow K^\pm \pi^+ \pi^-$ and $B^\pm \rightarrow K^\pm K^+ K^-$ decays with unprecedented precision [11]. The data sample is defined by a common kinematic selection of B^\pm decays to three charged mesons, followed by a PID selection to distinguish different final states. The raw asymmetries are obtained from fits to the invariant mass spectra, shown in Fig. 2, and are corrected for the variation of the acceptance efficiency in phase space. The inclusive CP asymmetries are then determined using Eq. (2), where the correction term A_Δ is found from a data control sample of $B^\pm \rightarrow J/\psi K^\pm$ decays. The inclusive CP asymmetries are calculated separately according to different trigger selections and then averaged to obtain

$$\begin{aligned}
 A_{CP}(B^\pm \rightarrow K^\pm \pi^+ \pi^-) &= 0.032 \pm 0.008 \text{ (stat)} \pm 0.004 \text{ (syst)} \pm 0.007(J/\psi K^\pm), \\
 A_{CP}(B^\pm \rightarrow K^\pm K^+ K^-) &= -0.043 \pm 0.009 \text{ (stat)} \pm 0.003 \text{ (syst)} \pm 0.007(J/\psi K^\pm),
 \end{aligned}$$

where the systematic uncertainties account for the signal and background fit models, trigger asymmetry and acceptance correction, and the last uncertainty is due to the CP asymmetry of the $B^\pm \rightarrow J/\psi K^\pm$ control channel [12]. The significances of the inclusive charge asymmetries are 2.8σ and 3.7σ , respectively. The latter represents the first evidence for an inclusive charge asymmetry in charmless three-body B decays.

The asymmetry distributions across the Dalitz planes of these two modes are also investigated. The background-subtracted Dalitz plots of the signal region are divided into bins with equal numbers of events, and an asymmetry variable is calculated between the number of negative and positive candidates in each bin, as shown in Fig. 3. The insets show the regions where large local asymmetries are concentrated. These appear to be positive for $B^\pm \rightarrow K^\pm \pi^+ \pi^-$, located at low $\pi^+ \pi^-$ invari-

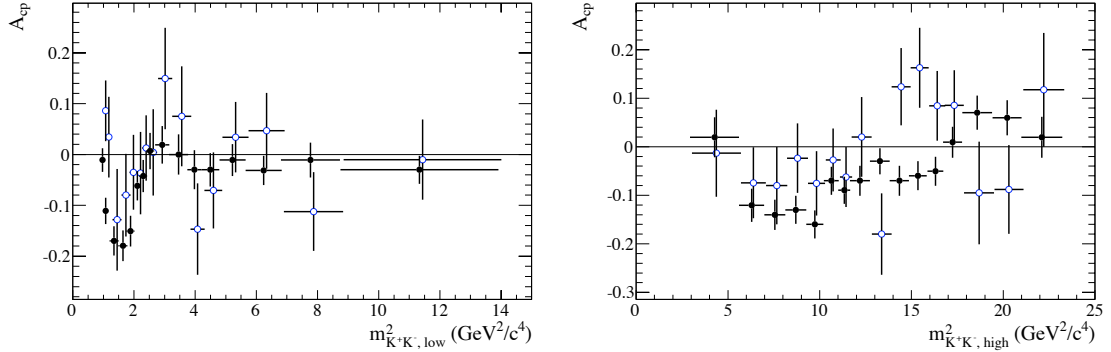


Figure 4: Asymmetry of $B^\pm \rightarrow K^\pm K^+ K^-$ decays as a function of (left) $m_{K^+K^-}^2$ low and (right) $m_{K^+K^-}^2$ high. The open points show BaBar measurements obtained using the $sPlot$ technique, and the solid points are A_{raw} distributions from LHCb.

ant masses below and around the $\rho(770)^0$ resonance, and above the $f_0(980)$ resonance. For $B^\pm \rightarrow K^\pm K^+ K^-$ the asymmetries are negative at low values of $m_{K^+K^-}^2$ low and $m_{K^+K^-}^2$ high, outside the $\phi(1020)$ resonance and in the region $1.2 < m_{K^+K^-}^2 \text{ low} < 2.0 \text{ GeV}^2/c^4$ devoid of resonances. The local CP asymmetries are measured from fits to the invariant mass spectra of candidates in two regions where large asymmetries are identified. The local charge asymmetries for the regions of $m_{K^\pm\pi^\mp}^2 < 15 \text{ GeV}^2/c^4$ and $0.08 < m_{\pi^+\pi^-}^2 < 0.66 \text{ GeV}^2/c^4$ for $B^\pm \rightarrow K^\pm\pi^+\pi^-$ decays, and $m_{K^+K^-}^2 \text{ high} < 15 \text{ GeV}^2/c^4$ and $1.2 < m_{K^+K^-}^2 \text{ low} < 2.0 \text{ GeV}^2/c^4$ for $B^\pm \rightarrow K^\pm K^+ K^-$ decays, are measured to be

$$A_{CP}^{\text{reg}}(K\pi\pi) = 0.678 \pm 0.078 (\text{stat}) \pm 0.032 (\text{syst}) \pm 0.007 (J/\psi K^\pm),$$

$$A_{CP}^{\text{reg}}(KKK) = -0.226 \pm 0.020 (\text{stat}) \pm 0.004 (\text{syst}) \pm 0.007 (J/\psi K^\pm).$$

The opposite-sign asymmetries between $B^\pm \rightarrow K^\pm\pi^+\pi^-$ and $B^\pm \rightarrow K^\pm K^+ K^-$, concentrated at low $\pi^+\pi^-$ and K^+K^- invariant masses, could be related to compound CP violation.

3.2 Comparison of $B^\pm \rightarrow K^\pm K^+ K^-$ results

A follow-up study of the amplitude analysis of $B^\pm \rightarrow K^\pm K^+ K^-$ decays [13] was performed by BaBar to compare the CP asymmetry distributions with the preliminary results obtained by LHCb [14]. The study [15] investigates the dependence of the CP asymmetry on the two-body K^+K^- invariant masses, shown in Fig. 4. The BaBar distributions show CP asymmetries obtained with the $sPlot$ technique, while the LHCb distributions show raw asymmetries from fits to the invariant mass spectra in bins of two-body masses, not corrected for detection and production asymmetries.

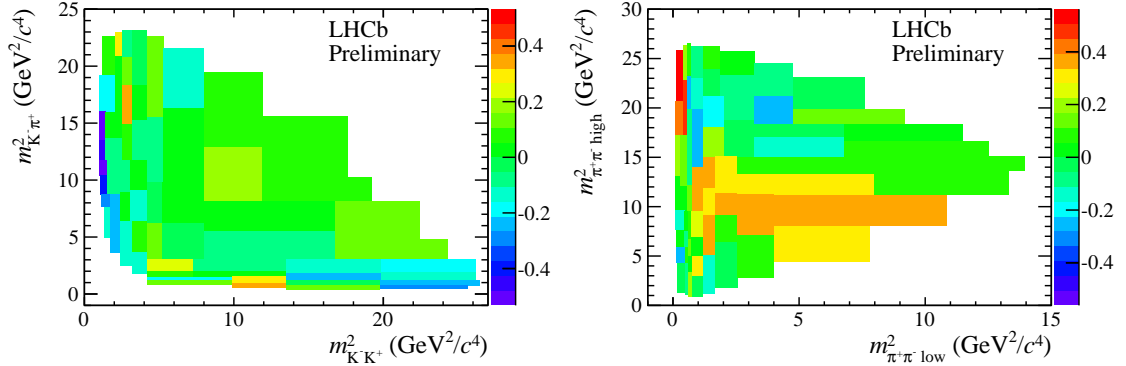


Figure 5: Asymmetries on the yields in bins of the Dalitz plane for (left) $B^\pm \rightarrow K^+K^-\pi^\pm$ and (right) $B^\pm \rightarrow \pi^+\pi^-\pi^\pm$.

Although the uncertainties on BaBar data are larger than those of LHCb, the patterns of the asymmetries agree well. For $m_{K^+K^-}^2$ low the asymmetries follow the same shape but seem to have a relative shift, which was observed to be flat across the spectrum and with an average value of $\Delta(\text{BaBar}-\text{LHCb}) = 0.045 \pm 0.021$. A similar positive and uniform shift of 0.053 ± 0.021 was measured from the $m_{K^+K^-}^2$ high distributions. These shifts are consistent with zero within 2 standard deviations, and are also consistent with the difference between the inclusive CP asymmetries obtained by BaBar and LHCb.

3.3 CP violation in $B^\pm \rightarrow K^+K^-\pi^\pm$ and $B^\pm \rightarrow \pi^+\pi^-\pi^\pm$ decays

The $B^\pm \rightarrow K^+K^-\pi^\pm$ and $B^\pm \rightarrow \pi^+\pi^-\pi^\pm$ modes are another set of channels with the same flavour quantum numbers, similar to $B^\pm \rightarrow K^\pm\pi^+\pi^-$ and $B^\pm \rightarrow K^\pm K^+K^-$, thus motivating a joint study. A preliminary measurement by LHCb [16] presents the inclusive CP asymmetries and their distributions in the Dalitz plots. The inclusive charge asymmetries are obtained analogously to the method described in Section 3.1 to be

$$\begin{aligned} A_{CP}(B^\pm \rightarrow \pi^+\pi^-\pi^\pm) &= 0.120 \pm 0.020 (\text{stat}) \pm 0.019 (\text{syst}) \pm 0.007(J/\psi K^\pm), \\ A_{CP}(B^\pm \rightarrow K^+K^-\pi^\pm) &= -0.153 \pm 0.046 (\text{stat}) \pm 0.019 (\text{syst}) \pm 0.007(J/\psi K^\pm), \end{aligned}$$

with significances of 4.2σ and 3.0σ , respectively. Both results represent the first evidences of inclusive charge asymmetries in these modes.

The asymmetry distributions of the numbers of events (containing signal and background) in bins of the Dalitz plots of the signal regions are shown in Fig. 5. For the $B^\pm \rightarrow K^+K^-\pi^\pm$ decay mode, a concentration of events, associated with negative asymmetries, is seen at low K^+K^- invariant masses, and was also studied in the event projections of the two-body invariant mass variables. This structure was already

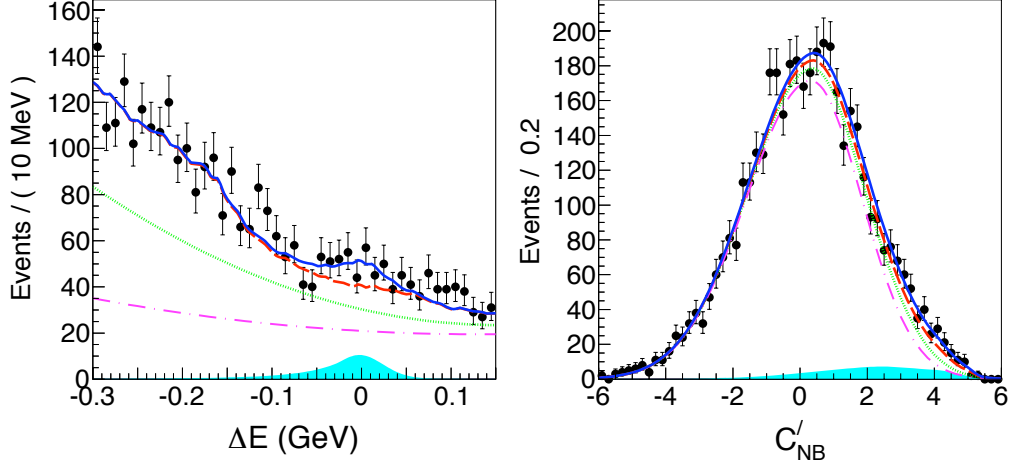


Figure 6: Projections of candidate events into (left) ΔE and (right) C'_{NB} . The solid blue curve shows the total PDF, the filled cyan region shows the signal, the dashed red curves the total background, the dotted green curves the continuum $q\bar{q}$ and generic $B\bar{B}$ background, and the dash-dotted magenta curves show the continuum $q\bar{q}$ background.

reported by BaBar [17], but its asymmetry was not studied. The large negative asymmetry seen by LHCb is not associated to resonances, as the $B^\pm \rightarrow K^\pm \pi^+ \pi^-$ mode does not have a $\phi(1020)$ contribution. For $B^\pm \rightarrow \pi^+ \pi^- \pi^\pm$ decays, a large positive asymmetry is identified at low $\pi^+ \pi^-$ invariant masses, below the $\rho(770)^0$ resonance. The local CP asymmetries of two regions, chosen as $m_{K^+ K^-}^2 < 1.5 \text{ GeV}^2/c^4$ for $B^\pm \rightarrow K^+ K^- \pi^\pm$ and $m_{\pi^+ \pi^-}^2 \text{ low} < 0.4 \text{ GeV}^2/c^4$ and $m_{\pi^+ \pi^-}^2 \text{ high} > 15 \text{ GeV}^2/c^4$ for $B^\pm \rightarrow \pi^+ \pi^- \pi^\pm$, are measured to be

$$\begin{aligned}
 A_{CP}^{\text{reg}}(B^\pm \rightarrow \pi^+ \pi^- \pi^\pm) &= 0.622 \pm 0.075 (\text{stat}) \pm 0.032 (\text{syst}) \pm 0.007 (J/\psi K^\pm), \\
 A_{CP}^{\text{reg}}(B^\pm \rightarrow K^+ K^- \pi^\pm) &= -0.671 \pm 0.067 (\text{stat}) \pm 0.028 (\text{syst}) \pm 0.007 (J/\psi K^\pm).
 \end{aligned}$$

The pattern of negative asymmetries at low $K^+ K^-$ masses and positive ones at low $\pi^+ \pi^-$ masses, not obviously related to resonances, repeats the one seen in $B^\pm \rightarrow K^\pm \pi^+ \pi^-$ and $B^\pm \rightarrow K^\pm K^+ K^-$ decays. These apparent correlations between the pairs of channels could be caused by the CPT constraint, and further studies need to take this possibility into account.

3.4 Evidence for the decay $B^0 \rightarrow K^+ K^- \pi^0$

A new measurement by Belle of the suppressed $B^0 \rightarrow K^+ K^- \pi^0$ decay [18] is presented. The data sample is selected using a neural network, and the signal yield is determined from an unbinned extended maximum likelihood fit to the two-dimensional

distributions of the energy difference, $\Delta E = \sum_i E_i - E_{\text{beam}}$, and a variable C'_{NB} related to the neural network output. The results of the fit are shown in Fig. 6.

From a signal yield of 299 ± 83 events, the branching fraction of the decay is obtained to be

$$\mathcal{B}(B^0 \rightarrow K^+ K^- \pi^0) = [2.17 \pm 0.60 (\text{stat}) \pm 0.24 (\text{syst})] \times 10^{-6}.$$

The dominant systematic uncertainties come from the π^0 detection efficiency and the efficiency variation over the Dalitz plane. The significance of the measurement, determined using a convolution of the statistical likelihood with a Gaussian function of width equal to the systematic errors, is 3.5σ , and constitutes the first evidence for the decay.

The $K^+ K^-$ and $K^+ \pi^0$ invariant mass distributions of the signal yields are studied to investigate the resonant structure of the decay. The distributions are obtained from fits in bins of the invariant masses. An excess of events is observed around 1.4 GeV in the $K^+ \pi^0$ invariant mass, but its interpretation would require higher statistics. The $K^+ K^-$ invariant mass distribution does not allow a definitive statement about a possible structure similar to the one seen in $B^\pm \rightarrow K^+ K^- \pi^\pm$ decays by BaBar [17] and LHCb [16].

3.5 Branching fraction measurements of $B^\pm \rightarrow p\bar{p}K^\pm$ decays

The $B^\pm \rightarrow p\bar{p}K^\pm$ decay mode allows the study of $c\bar{c}$ states and charmonium-like mesons that decay to $p\bar{p}$. The branching fractions of the decay $B^\pm \rightarrow p\bar{p}K^\pm$ for different intermediate states have been measured by LHCb [19]. The event selection is based on a boosted decision tree algorithm. The signal yields of the different resonant components are obtained from fits to the $p\bar{p}$ invariant mass distributions within a B mass signal window. The fit results are shown in Figs. 7 and 8.

The branching fractions of the contributions shown in the figures are obtained relative to the one of the J/ψ intermediate state,

$$\begin{aligned} \frac{\mathcal{B}(B^\pm \rightarrow p\bar{p}K^\pm)_{\text{total}}}{\mathcal{B}(B^\pm \rightarrow J/\psi K^\pm \rightarrow p\bar{p}K^\pm)} &= 4.91 \pm 0.19 (\text{stat}) \pm 0.14 (\text{syst}), \\ \frac{\mathcal{B}(B^\pm \rightarrow p\bar{p}K^\pm)_{M_{p\bar{p}} < 2.85 \text{ GeV}/c^2}}{\mathcal{B}(B^\pm \rightarrow J/\psi K^\pm \rightarrow p\bar{p}K^\pm)} &= 2.02 \pm 0.10 (\text{stat}) \pm 0.08 (\text{syst}), \\ \frac{\mathcal{B}(B^\pm \rightarrow \eta_c(1S)K^\pm \rightarrow p\bar{p}K^\pm)}{\mathcal{B}(B^\pm \rightarrow J/\psi K^\pm \rightarrow p\bar{p}K^\pm)} &= 0.578 \pm 0.035 (\text{stat}) \pm 0.025 (\text{syst}), \\ \frac{\mathcal{B}(B^\pm \rightarrow \psi(2S)K^\pm \rightarrow p\bar{p}K^\pm)}{\mathcal{B}(B^\pm \rightarrow J/\psi K^\pm \rightarrow p\bar{p}K^\pm)} &= 0.080 \pm 0.012 (\text{stat}) \pm 0.009 (\text{syst}). \end{aligned}$$

The results are compatible with world average values. An upper limit on the relative branching fraction of B^\pm into the $X(3872)$ state is also obtained.

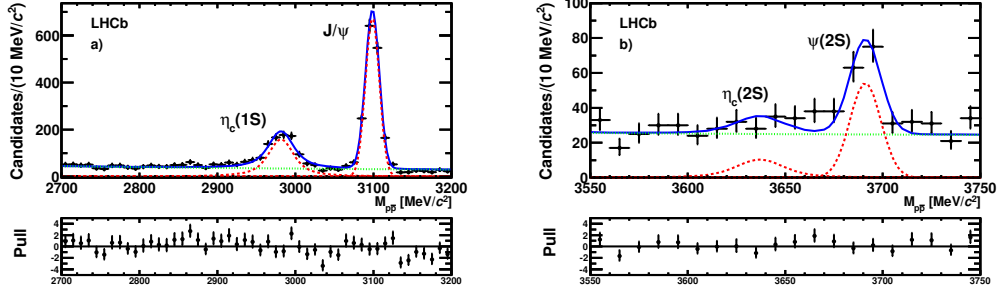


Figure 7: Invariant mass distribution of the $p\bar{p}$ system in the regions around (a) the $\eta_c(1S)$ and J/ψ and (b) the $\eta_c(2S)$ and $\psi(2S)$ states.

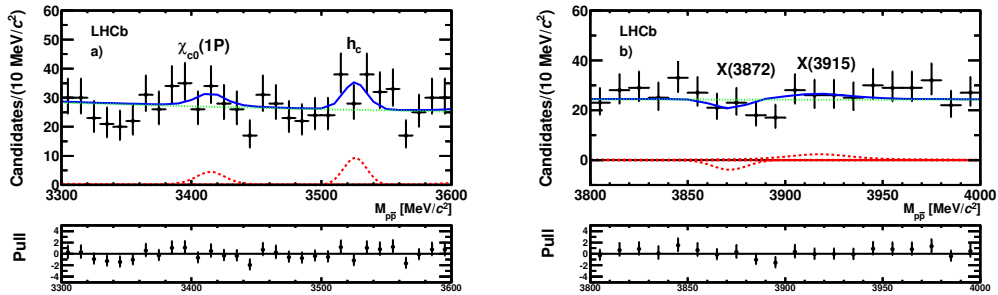


Figure 8: Invariant mass distribution of the $p\bar{p}$ system in the regions around (a) the $\chi_{c0}(1P)$ and h_c and (b) the $X(3872)$ and $X(3915)$ states.

4 Observation of the decay $B_s^0 \rightarrow \phi \bar{K}^{*0}$

B meson decays to two vector mesons that proceed only through penguin diagrams are sensitive to new physics contributions in the loops. They also offer the possibility to study angular distributions and polarisation fractions. LHCb has recently claimed the first observation of the $B_s^0 \rightarrow \phi \bar{K}^{*0}$ decay mode [20]. The data selection reconstructs the final states $B_s^0 \rightarrow \phi(K^+K^-)\bar{K}^{*0}(K^-\pi^+)$ using a geometrical-likelihood multivariate analysis. The signal yield is obtained from an unbinned extended maximum likelihood fit to the invariant mass spectrum, shown in Fig. 9, resulting in 30 ± 6 events. The statistical significance of the yield is calculated from a likelihood ratio test. With a significance of 6.1σ , this measurement represents the first observation of the $B_s^0 \rightarrow \phi \bar{K}^{*0}$ decay mode.

The branching fraction of the decay is measured using $B^0 \rightarrow \phi K^{*0}$ as a normalisation channel to be

$$\mathcal{B}(B_s^0 \rightarrow \phi \bar{K}^{*0}) = [1.10 \pm 0.24 (\text{stat}) \pm 0.14 (\text{syst}) \pm 0.08 (f_d/f_s)] \times 10^{-6},$$

where the third uncertainty is due to the uncertainty on the ratio of b -hadron production fractions f_d/f_s [21]. The main systematic uncertainties are due to the fit model

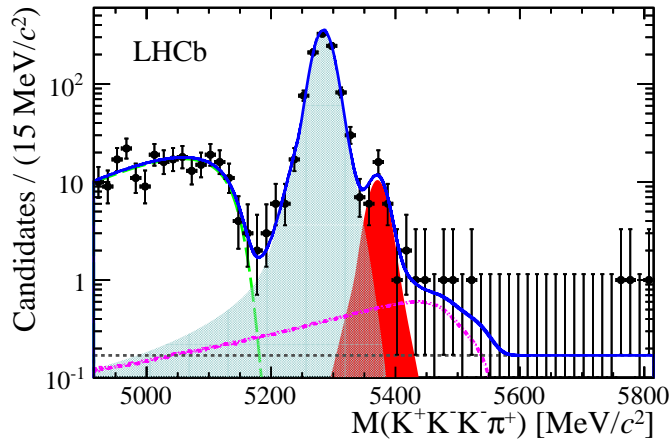


Figure 9: Fit to the $KKK\pi$ invariant mass spectrum, with the $B_s^0 \rightarrow \phi\bar{K}^{*0}$ signal given by the filled red area.

and the purity of the resonance components.

An untagged time-integrated polarisation analysis of the angular distributions is performed to obtain the polarisation fractions of the decay. The longitudinal polarisation fraction is measured to be

$$f_0 = 0.51 \pm 0.15 \text{ (stat)} \pm 0.07 \text{ (syst)}.$$

The result agrees with that of the $b \rightarrow s$ penguin decay $B^0 \rightarrow \phi K^{*0}$ [22].

5 Conclusions

Several recent results from studies of charmless B decays were reported. Branching fraction measurements include the first observation of $B_s^0 \rightarrow \phi\bar{K}^{*0}$ decays and the first evidence for $B^0 \rightarrow K^+K^-\pi^0$ decays. The first observation of direct CP violation in B_s^0 decays was presented, as well as evidences for inclusive charge asymmetries in three-body B^\pm decays. Interesting patterns of CP violation in three-body charmless B^\pm decays were observed by LHCb. Further experimental studies are needed to resolve the difference between the CP asymmetries of $B^\pm \rightarrow K^\pm K^+ K^-$ seen by BaBar and LHCb.

ACKNOWLEDGEMENTS

I am grateful to the CBPF and the organising committee of FPCP-2013 for funding my participation in the conference.

References

- [1] A. A. Alves Jr. *et al.* [LHCb Collaboration], “The LHCb detector at the LHC”, JINST **3** (2008) S08005.
- [2] B. Aubert *et al.* [BaBar Collaboration], “The BaBar detector,” Nucl. Instrum. Meth. A **479** (2002) 1, arXiv:hep-ex/0105044.
- [3] A. Abashian *et al.*, “The Belle detector”, Nucl. Instrum. Meth. A **479** (2002) 117.
- [4] R. Aaij *et al.* [LHCb Collaboration], “First observation of CP violation in the decays of B_s^0 mesons”, Phys. Rev. Lett. **110** (2013) 221601, LHCb-PAPER-2013-018, arXiv:1304.6173 [hep-ex].
- [5] M. Adinolfi *et al.*, “Performance of the LHCb RICH detector at the LHC,” Eur. Phys. J. C **73** (2013) 2431, arXiv:1211.6759 [physics.ins-det].
- [6] R. Marshak, Riazuddin and C. Ryan, “Theory of weak interactions in particle physics”, Wiley-Interscience, New York, USA, 1969.
- [7] L. Wolfenstein, “Final state interactions and CP violation in weak decays”, Phys. Rev. D **43** (1991) 151.
- [8] G. C. Branco, L. Lavoura and J. P. Silva, “ CP Violation”, Int. Ser. Monogr. Phys. **103** (1999) 1.
- [9] I. I. Y. Bigi and A. I. Sanda, “ CP violation”, Camb. Monogr. Part. Phys. Nucl. Phys. Cosmol. **9** (2000) 1.
- [10] H. -Y. Cheng, C. -K. Chua and A. Soni, “Final state interactions in hadronic B decays”, Phys. Rev. D **71** (2005) 014030, arXiv:hep-ph/0409317.
- [11] R. Aaij *et al.* [LHCb Collaboration], “Measurement of CP violation in the phase space of $B^\pm \rightarrow K^\pm \pi^+ \pi^-$ and $B^\pm \rightarrow K^\pm K^+ K^-$ decays”, LHCb-PAPER-2013-027, arXiv:1306.1246 [hep-ex].
- [12] J. Beringer *et al.* (Particle Data Group), Phys. Rev. D **86** (2012) 010001.
- [13] B. Aubert *et al.* [BaBar Collaboration], “Dalitz plot analysis of the decay $B^\pm \rightarrow K^\pm K^\pm K^\mp$ ”, Phys. Rev. D **74** (2006) 032003, arXiv:hep-ex/0605003.
- [14] R. Aaij *et al.* [LHCb Collaboration], “Evidence for CP violation in $B^\pm \rightarrow K^\pm \pi^+ \pi^-$ and $B^\pm \rightarrow K^\pm K^+ K^-$ decays”, LHCb-CONF-2012-018.

- [15] J. P. Lees *et al.* [BaBar Collaboration], “Study of the K^+K^- invariant-mass dependence of CP asymmetry in $B^+ \rightarrow K^+K^-K^+$ decays”, SLAC-PUB-154451, arXiv:1305.4218 [hep-ex].
- [16] R. Aaij *et al.* [LHCb Collaboration], “Evidence for CP violation in $B^\pm \rightarrow \pi^\pm\pi^+\pi^-$ and $B^\pm \rightarrow K^+K^-\pi^\pm$ decays”, LHCb-CONF-2012-028.
- [17] B. Aubert *et al.* [BaBar Collaboration], “Observation of the Decay $B^+ \rightarrow K^+K^-\pi^+$ ”, Phys. Rev. Lett. **99** (2007) 221801, arXiv:0708.0376 [hep-ex].
- [18] V. Gaur *et al.* [Belle Collaboration], “Evidence for the decay $B^0 \rightarrow K^+K^-\pi^0$ ”, Phys. Rev. D **87** (2013) 091101, arXiv:1304.5312 [hep-ex].
- [19] R. Aaij *et al.* [LHCb Collaboration], “Measurements of the branching fractions of $B^+ \rightarrow p\bar{p}K^+$ decays”, Eur. Phys. J. C **73** (2013) 2462, LHCb-PAPER-2012-047, arXiv:1303.7133 [hep-ex].
- [20] R. Aaij *et al.* [LHCb Collaboration], “First observation of the decay $B_s^0 \rightarrow \phi\bar{K}^{*0}$ ”, LHCb-PAPER-2013-012, arXiv:1306.2239 [hep-ex].
- [21] R. Aaij *et al.* [LHCb Collaboration], “Determination of f_s/f_d for 7 TeV pp collisions and a measurement of the branching fraction of the decay $B_d \rightarrow D^-K^+$ ”, Phys. Rev. Lett. **107** (2011) 211801, arXiv:1106.4435 [hep-ex].
- [22] B. Aubert *et al.* [BaBar Collaboration], “Time-dependent and time-integrated angular analysis of $B \rightarrow \phi K_s^0\pi^0$ and $B \rightarrow \phi K^+\pi^-$ ”, Phys. Rev. D **78** (2008) 092008, arXiv:0808.3586 [hep-ex].